Corrosion evaluation and prevention of reactor materials to contain thermochemical material for thermal energy storage

Aran Solé[1], Camila Barreneche[1,2], Ingrid Martorell[1,3], Luisa F. Cabeza[1,*]

[1]GREA Innovació Concurrent, Universitat de Lleida, Lleida, Spain. Edifici CREA, Pere de Cabrera s/n, 25001, Lleida, Spain. Tel.: +34-973 003576; Fax: +34-973 003575. *lcabeza@diei.udl.cat

[2]Department of Materials Science & Metallurgical Engineering, Universitat de Barcelona, Martí i Franqués 1-11, 08028 Barcelona, Spain

[3]Serra Húnter Fellow

*Corresponding author: lcabeza@diei.udl.cat

Abstract

Thermochemical materials (TCM) can be used for seasonal heat storage, storing high amounts of thermal energy coming from the sun in summer and releasing it in winter, when heating for houses is needed. One promising TCM for building comfort applications is the Na_2S/water pair due to its high energy density and appropriate reaction temperature that can be achieved by a solar collector. Nonetheless, Na_2S reacts with oxygen and is corrosive to metals, especially with those used to build up heat exchangers or reactors that contain the TCM. Therefore, corrosion tests in a self-developed experimental setup under vacuum conditions, 13 mbar, between $Na_2S \cdot 9H_2O/5H_2O$ and two reactor metals: copper and stainless steel 316 have been performed. Since copper is corroded and is highly used for thermochemical reactors, two promising coatings, Halar and electroless nickel, have been applied. Furthermore, aluminium has also been tested coated with these coatings. Halar is a potential candidate to protect both copper and aluminium heat exchangers/reactor that may contain Na_2S/H_2O pair for thermochemical energy storage. Stainless steel 316 is also corrosion resistant to the selected TCM.

Keywords: Corrosion; Thermal energy storage (TES); Thermochemical material (TCM); Sodium sulphide; Vacuum reactor; Coatings.

1. Introduction

Thermal energy storage (TES) is extremely necessary to match the energy available and the demand. This could lead to thermally independent houses, which would have a positive effect in reducing the global CO_2 emissions. The research in this field is mainly focused on the storage medium and how to implement it in the most efficient way. Several storage materials have been studied, based on different concepts. Sensible, phase change and thermochemical materials are being used to fulfil energy storage requirements depending on the application [1, 2].

In this paper the focus is on thermochemical materials (TCM) which undergo a chemical reversible reaction to store and release energy. TCM is an emerging energy storage media with the potential for high-density leading to compact thermal energy storage systems [3] and for high energy efficient systems for energy conversion [4]. Moreover, those materials present a huge advantage which remains in almost zero thermal losses to the ambient, since the energy is stored in the form of chemical bonds. Therefore, TCM are suitable for seasonal storage, meaning to provide heat in winter that has been charged in summer. On the other hand, one of the major drawbacks of TCM is that they are corrosive to the reactor/heat exchanger material, usually metal based.

Corrosion causes big investment costs, results of one study show that the total annual estimated direct cost of corrosion in the U.S. is a staggering $276 billion, approximately 3.1% of the nation's Gross Domestic Product (GDP) [5]. Hence, corrosion tests should be performed before to ensure long term performance of the equipment containing TCM [6, 7].

In a previous study [7] results coming from an experimental corrosion test simulating an open TCM reactor between several TCM and common vessel metals were published. TCM reactors can be open or closed, integrated or non-integrated [8]. Open reactors take the water vapour from the atmospheric air while closed reactors imply that water circulates in a closed loop and is taken from an evaporator and released to a condenser. The later ones can operate under lower or vacuum pressures or inert atmospheres.

Some of the most studied TCM work better under low pressures [9] or in an inert or vacuum atmosphere when side reactions have to be controlled [10]. No literature has been found concerning corrosion vacuum tests with TCM. One of the moving forward-preventive strategies for corrosion costs savings is to promote research [5] and thus

66 perform tests seeking for compatible materials and/or preventive solutions like applying
67 coatings [11, 12].

68 There are several types of coating that can protect almost all metals available for
69 engineering use from air, water, acid corrosion, saline ambient, etc. [13]. Those coating
70 are mainly classified as organic [14] and inorganic coatings [15] and the method used
71 to coat the substrates is the main issue under study at this moment.

72 The aim of this study is to develop a device to test corrosion between TCM and metals,
73 under vacuum and controlled temperature. Moreover, experimental corrosion tests
74 have been performed in this setup looking for the suitable material to build up vessels
75 or reactors which contain Na_2S/H_2O pair as a thermochemical energy storage material.

76 From the recent literature published in this field [1,3,7,8,12] it can be withdrawn the
77 need of more research in order to overcome TCM issues like corrosion, compaction,
78 stability, etc. to promote this technology towards market availability. The contribution of
79 the present study is essential for the design of a reactor/heat exchanger where a TCM
80 reaction for building applications takes place. Although it has been focused on a
81 specific working pair, the designed methodology and setup address a specific step in
82 the reactor design procedure when selecting metals to work in contact with TCM.

83

84 **2. Setup and methodology**

85 **2.1 Setup**

86 The present setup is designed and built to perform corrosion tests simulating closed
87 and integrated TCM reactors. Glass has been selected for being an inert material able
88 to stand high temperatures, low pressures, and allowing direct visual inspection. The
89 design was thought to obtain a versatile, multifunctional device which can operate
90 under a wide range of pressures, temperatures, and different atmospheres, therefore
91 several TCM.

92 A general view of the setup is shown in Figure 1. It consists of a 5 L glass jacketed
93 reactor, connected to a heating unit (thermostatic water bath), an evaporator (round-
94 bottom flask), and a vacuum pump from Vacuubrand PC 600 series. Tubing from the
95 reactor to the vacuum pump is polyamide based connected with common clamps. The
96 reactor contains one open 300 ml vessel to place the TCM and the specimens to be
97 tested (see Figure 2). One temperature sensor is giving the TCM temperature, and
98 another is placed in the atmosphere. Relative humidity (RH) is also measured on-line

101   with a HygroPalm HP22-A. Furthermore, total pressure is measured and controlled by
102   the vacuum pump.

105   The vacuum pump runs in continuous mode, to assure vacuum inside the reactor. The
106   vacuum pump presents an outlet for venting gases, which is directed to the fume hood,
107   being cooled previously (cooling unit) to collect condensed outlet water vapour and
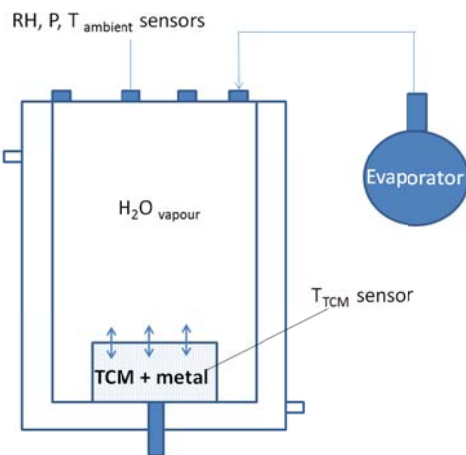108   other condensable gases.

106

107
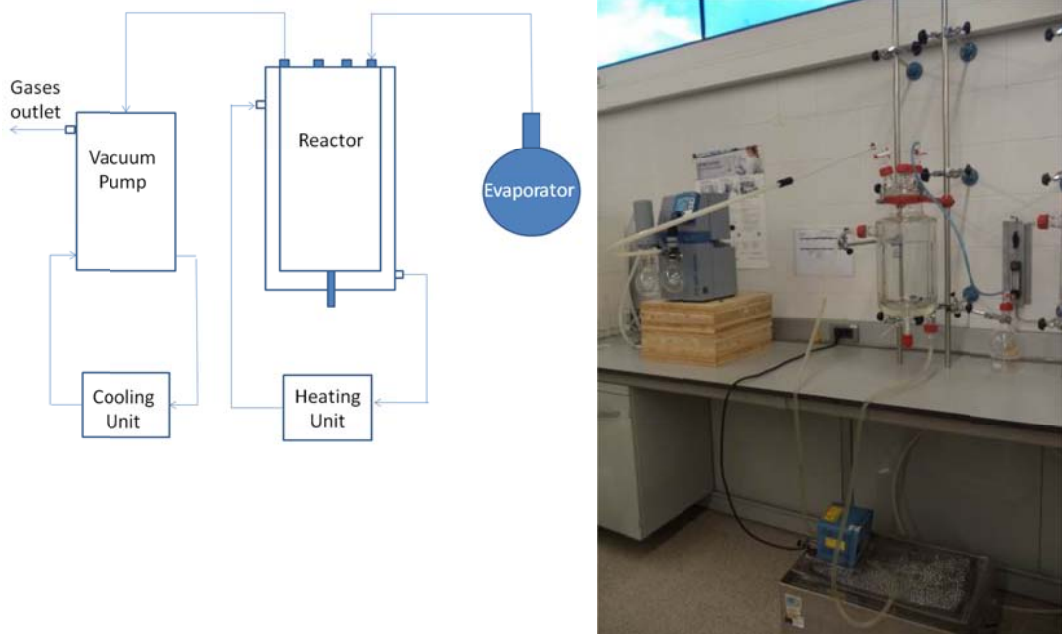
108   **Figure 1. General view of the setup. Left: scheme, right: picture.**
109

110

111   **Figure 2. Reactor and evaporator setup sketch.**

112

2.2 Methodology

For each metal sample, four specimens are needed. One is the reference and the other three are tested for a week in contact with the TCM. The three specimens are replicates in order to ensure the repeatability of the experiments.

To evaluate the results, a methodology accordingly to the setup has been designed. Two different methodologies, one for the single metal specimen and one for the coated metals, are detailed here. First, the metal specimen are cleaned (no polished, no brushed, only acetone). Then, they are weighted in a precision balance (± 0.01 mg) AG135 from Mettler-Toledo and are visually observed by a Zwek optical microscope. The coated specimen are weighted in the same precision balance, but observed in an ESEM Quanta 200 FEI, XTE 325/D8395 scanning electronic microscope (SEM). An SEM is needed for the coated samples since more precision and resolution is required to measure the coating thickness. At this point the methodology merges and three specimens of each sample are placed inside the reactor in a 300 ml vessel fully in contact with the solid $Na_2S \cdot 9H_2O$. An immersion corrosion test following ASTM G1 [16], under the specified operating conditions determined by the TCM selected, is performed for a week. Before vacuum the reactor, nitrogen gas flows through it to make sure there is no oxygen inside. Finally, the heating unit is connected and set to the established set point.

After the corrosion test, the three specimens are visually inspected, weighted in the same balance and observed in the appropriate microscope. Corrosion processes that go further than the surface level can be identified by both microscopes. Therefore, vessel materials that are not appropriate can be identified. Also, TCM characterization after corrosion tests should be performed (i.e. XRD) to identify the reaction process of the TCM and other possible chemicals.

On the other hand, previous tests were performed to ensure vacuum tightness in the reactor and to check the start-up of the reactor as well as to conduct it to established steady state conditions. Then, tests with only TCM have to be conducted to see the behaviour of the TCM without possible products from corrosion reaction.

The methodology to evaluate corrosion is based on ASTM G1. Corrosion rates are obtained using equation 1 for single metals since ASTM G1 is not adapted to coated metals. Mass loss corresponds to the decrease in mass between before and after (after chemical cleaning, see ASTM G1) the corrosion test.

146

$$CR = \frac{\Delta m}{A \cdot (t_o - t_f)}$$

Eq. 1

147 Corrosion rate CR (mg/cm^2·yr) takes into account the mass loss (Δm), the contact area
148 of the metal specimen (A), and the time of exposure (t_0-t_f).

149

150 **3. Materials**

151 **3.1 TCM**

152

153 A promising TCM, mainly seeking high energy density, has been selected to test and
154 validate the new experimental setup. Sodium sulphide and water pair (Na_2S/H_2O) as a
155 TCM presents a net energy storage value (see Table 1) which is within the best salt
156 hydrates for building applications [17, 18]. Its main drawbacks according to the hazard
157 statements of the Regulation (Ec) 1272/2008 are: toxic if swallowed, it may be
158 corrosive to metals, and in contact with acids liberates toxic gas (H_2S) [19]. Swallowing
159 it can be avoided if the material is kept in a closed vessel as the one designed here.
160 Corrosion can be prevented by coating the metal in contact as it is done in this work.
161 Furthermore, an inert atmosphere or vacuum is needed to prevent sulphites formation
162 and this is why the experimental setup is designed to work under vacuum conditions.

163 The purchased sodium sulphide nonahydrate ($Na_2S \cdot 9H_2O$) is manufactured by Alfa
164 Aesar with 98.0 % purity. Properties associated to the chosen TCM reaction are shown
165 in Table 1.

166 The reaction from nonahydate to pentahydrate accomplishes the requirement for
167 building applications, a reaction temperature below 100-150 ºC achievable by solar
168 collectors and promising net enthalpy values, as shown in Table 1.

169

170 **Table 1. TCM reaction properties for the corrosion vacuum tests.**

$Na_2S \cdot 9H_2O(s) \rightarrow Na_2S \cdot 5H_2O(s) + 4H_2O(v)$	nonahydrate	pentahydrate	Ref
CAS number	1313-84-4	1313-83-3	[19]
Density (g/cm³)	1.43	1.58	[17]
Melting temperature (ºC)	49	83	[17, 20]
Molecular weight (g/mol)	240.184	168.122	[21]

Extrapolated onset temperature (ºC)	32.5	[20]
ΔH_r (KJmol^{-1})	215±20	[20]
$\Delta H_{net,V*}$ (KWhm^{-3})	133	[17]

*Includes the volume of the water in the water storage tank

The reactor operating conditions, which are given by the TCM reaction itself [20], are shown in Table 2. Everything runs in continuous mode. Water vapour pressure is always as expected since it is taken from the external evaporator, which is also under vacuum. Water vapour pressure is also checked by measuring RH and calculating saturated pressure by Clausius-Clapeyron equation.

Table 2. Reactor test operating conditions.

Water vapour pressure (mbar)	13
Reactor temperature (ºC)	32.5 (dehydration)
Evaporator temperature (ºC)	10

3.2 Metals and coated metals

The absorption and release of energy coming from the TCM reaction takes place in reactors. Therefore, heat transfer is needed to be promoted from the TCM to the heat transfer fluid, usually water for building applications. In that sense prototypes are being made of high conductivity metals, such as: copper, aluminium, or even stainless steel 316.

It is known that there are several materials to be avoided in contact with Na_2S: acids, oxidizing agents, water/moisture, aluminium/aluminium alloys, copper and air [22].

In this paper single metals under study are stainless steel 316 and copper. Moreover, coatings are considered to protect copper and aluminium from Na_2S corrosion. Two different coatings were chosen, halar (organic coating) and electroless nickel (inorganic coating). All the pieces dimensions are 6 x 6 x 0.2 cm.

Halar® is an organic coating which is mainly composed by Ethylene Chloro Trifluoroethylene (ECTFE). At temperatures up to 120 °C the polymer is

197 neither affected by stress cracking nor attacked by the majority of chemical reagents.
198 ECTFE is resistant to most chemicals except chlorinated solvents and has better
199 barrier properties to SO_2, Cl_2, HCl, and water than fluorinated ethylene propylene (FEP)
200 and polyvinylidene fluoride (PVDF) [23]. These coatings can be applied with
201 electrostatic powder coating or with spray coating in the slurry formulation which have
202 been described by Choy [24].

204 Electroless autocatalytic Nickel-Phosphorus Coatings, from now on electroless nickel,
205 are alloys of nickel and phosphorus produced by autocatalytic chemical reduction with
206 hypophosphite and generally deposited from acid solutions operating at high
207 temperatures. These coatings have multifunctional properties, such as hardness, heat
208 hardenability, abrasion, wear and corrosion resistance, magnetics, electrical
209 conductivity provides diffusion barrier, and solderability [25]. A finishing based on an
210 anticorrosive spray has also been applied onto one copper sample to see if it acts as a
211 protective film against Na_2S.

213 **4. Results and discussion**

214 Obtained results from the corrosion test performed to the abovementioned specimen
215 are gathered and shown by, first, single metal specimen which are copper and
216 stainless steel 316, and secondly, by the coated specimen.

218 **4.1 Metal specimen**
219   **A) Copper**

220 Corrosion signs were clearly observed in copper specimens, as it can be seen in
221 Figure 3. Black spots (i.e. CuS or/and Cu_2S) on the surface which are products from a
222 side reaction can be clearly observed. The three last pictures (Figure 3, bottom) are
223 from the same specimens after chemical cleaning (following ASTM G1). They present
224 no solid products from corrosion process, but still some surface damage is seen since
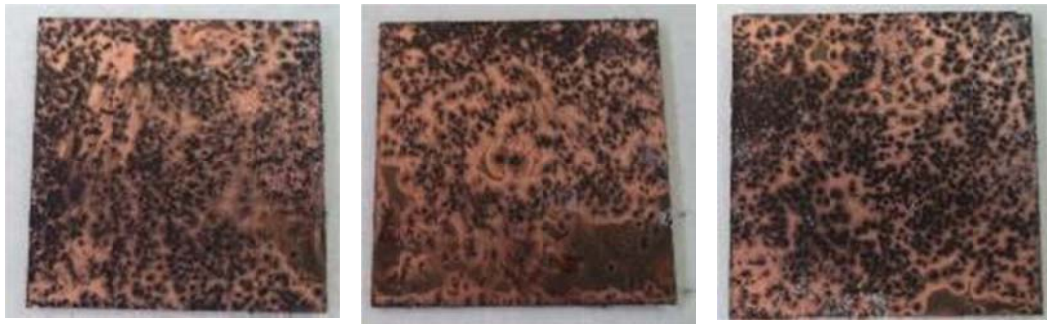225 the surface colour is deteriorated when compared to the initial copper specimen.

233

Specimen before chemical cleaning process (after corrosion test)

Specimen after chemical cleaning process

234

235   **Figure 1. Copper specimen after one week corrosion test with Na_2S. Top: before and bottom: after cleaning.**

236

239   The microscopic section images of the specimen (Figure 4) denote there is no

240   corrosion further than the surface. The lines are due to the cutting process of the

241   specimen.

240

241   **Figure 2. Copper section microscopic images before (left) and after (right) corrosion test.**

242

246   Corrosion rates (CR) are listed in Table 3. These values of CR belong to the not

247   recommended range (50-99 mg cm^{-2} yr^{-1}) for service greater than a year (see Table 4).

248   When comparing these values with the previously obtained [7] in atmospheric pressure

249   and humidity conditions, it can be concluded that in vacuum, CR value is reduced

around 30 times. Nonetheless, for this application copper is not recommended to contain Na_2S/H_2O, neither in open nor in close configurations. For that reason, it is remarkable that a coating is needed to protect it before its implementation as part of a system containing this TCM.

Table 3. Initial and final weight of the Cu specimen under study and calculated CR.

	Initial weight (g)	Final weight (g)	CR (mg cm^{-2} yr^{-1})
Specimen 1	63.694	63.609	85.54
Specimen 2	63.681	63.601	80.14
Specimen 3	63.727	63.646	81.11

Table 2. Guide for corrosion weight loss used in the industry [26].

mg/cm^{2}yr	Recommendation
>1000	Completely destroyed within days
100–999	Not recommended for service greater than a month
50–99	Not recommended for service greater than 1 yr
10–49	Caution recommended, based on the specific application
0.3–9.9	Recommended for long term service
<0.2	Recommended for long term service; no corrosion, other than as a result of surface cleaning, was evidenced

B) Stainless steel 316

Stainless steel 316 did not show corrosion signs after the test. Specimens have the same appearance as before testing. There are not corrosion effects on the surface. Moreover, microscopic images (see Figure 5) show that there are not corrosion points on the surface of the specimens under study. There is no difference at microscope scale regarding the section surface of the stainless steel specimens under study, either.

Specimens before corrosion test

Specimens after corrosion test

266 **Figure 5. Stainless steel 316 specimens after one week corrosion test with Na$_2$S. Microscopic images before**
267 **(top) and after (bottom) corrosion test.**

267

272 Corrosion rate values are shown in Table 5, which are inside recommended range for
273 long term service (see Table 4). CR values in this case are in the same range as the
274 obtained under atmospheric pressure and humidity conditions [7]. Therefore, stainless
275 steel 316 corrosion compatibility with Na$_2$S/H$_2$O is not influenced by the working
276 atmosphere (e.g. air and vacuum).

273

274 **Table 3. Initial and final weight of the stainless steel 316 specimens under study and calculated CR.**

	Initial weight (g)	Final weight (g)	CR (mg cm^{-2} yr^{-1})
Specimen 1	80.804	80.800	4.34
Specimen 2	81.046	81.041	5.05
Specimen 3	80.883	80.878	4.44

275

282 Stainless steel 316 is a potential candidate as it has been experimentally tested under
283 the real operating conditions and the results recommend it for long term service;
284 nevertheless there are also other aspects to take into account when selecting a
285 material vessel to build up a heat exchanger or a reactor. Heat transfer should not be
286 limiting in a TCM reactor since then thermal power output of the reactor/heat
287 exchanger would be lower than expected. Since a coating layer represents an
288 additional thermal resistance in the heat transfer during reaction, experiments are

282   suggested to be carried out to reveal to which extent the thermal performance of the

283   heat exchanger is decreased by the coating.

284

285   **4.2 Coated specimens: halar® and electroless nickel**

286   **A) Copper coated with halar®**

287

288   Figure 6 shows the SEM images captured for each Cu-specimen tested under vacuum

289   corrosion test and one reference. The images correspond to the cross section of the

290   specimens under study where the halar® coating can be seen in the upper side.

291   SEM images revealed that the coating thickness remains constant and is exactly the

292   same (around 190-200 µm) as it is observed in Figure 6. The coating thickness

293   remains almost constant regardless of the specimen. Therefore, copper coated with

294   halar® is corrosion resistant to Na_2S/H_2O pair and can be used when copper is needed

295   as a base metal.

296

297

298

299

300

301

302

303

304

305

306

307

308
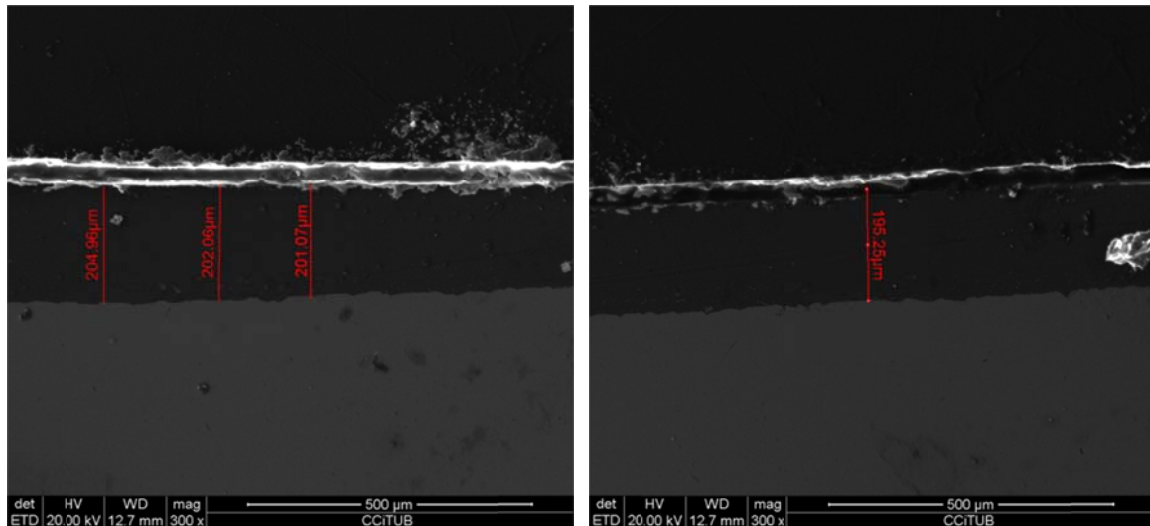
Reference   Specimen 1
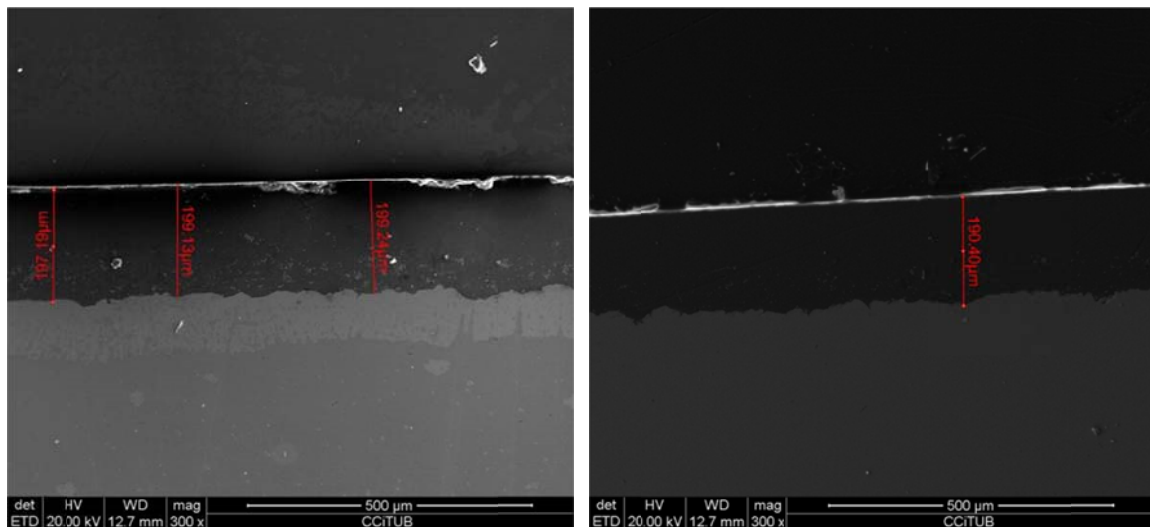
Specimen 2   Specimen 3
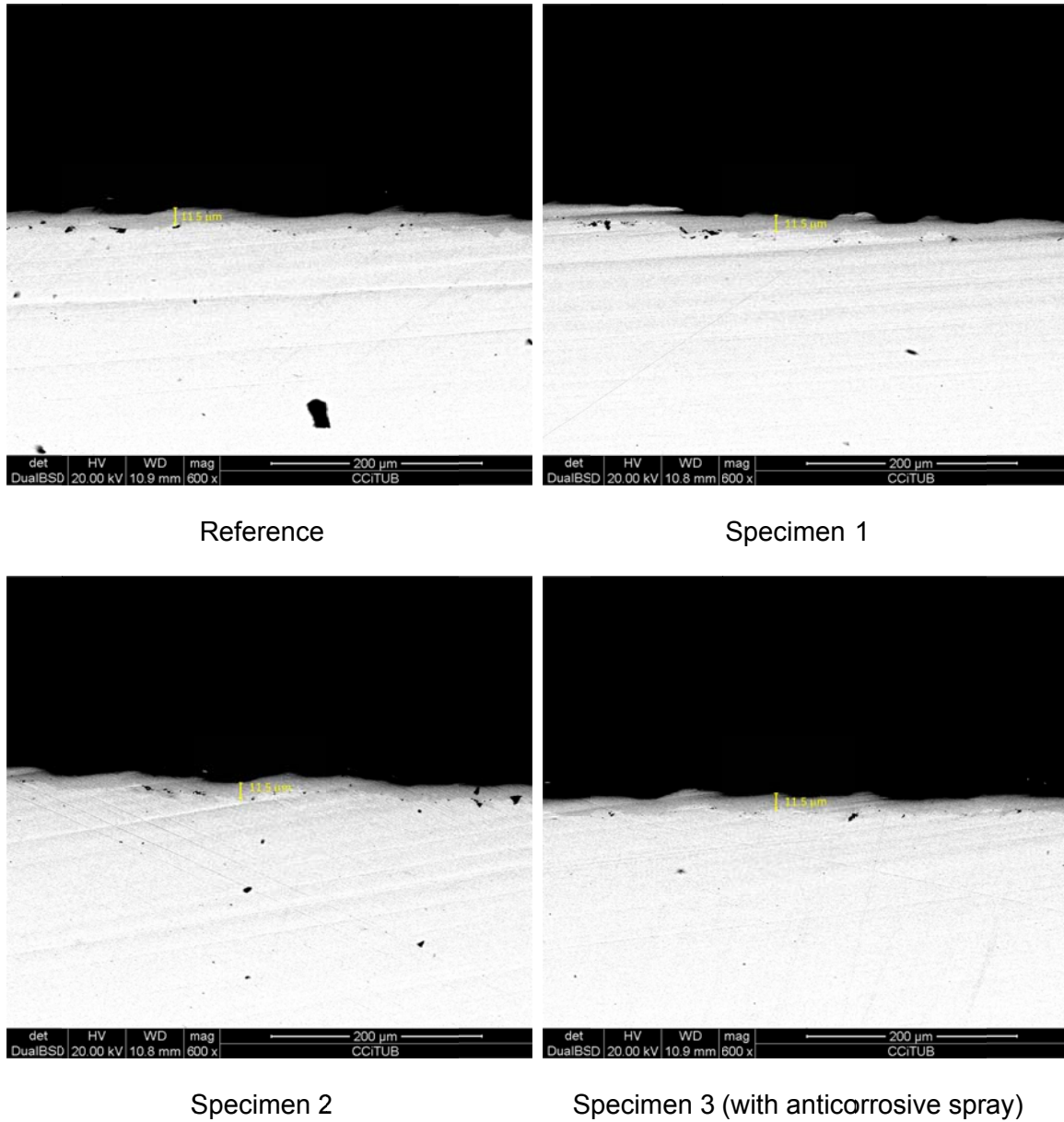
Figure 6. Copper specimens coated with halar®.

B) Copper coated with electroless nickel

Figure 7 shows the coating of the specimens coated with Ni-electroless technique. There is one specimen without being tested (the reference), there are two specimens coated with Ni-electroless coating and there is one specimen that has the same coating and also a finish anticorrosive and non-sticked spray (M3). The samples morphology is shown in the SEM using secondary electrons. However, the backscattered electrons are able to provide composition information of the displayed sample: the darker the sample the lighter the atoms are. Thus, the morphology of the Aluminium + electroless Ni samples is very similar and secondary electrons are unable to differentiate the sample and the coating. In addition, backscattered electrons not clarify much the difference between sample and coating because Ni and Al have very similar atomic weight. Thereby, SEM images are not very enlightening, although the thickness of the coating layer is distinguished. Figure 7 shows that there is no corrosion and the
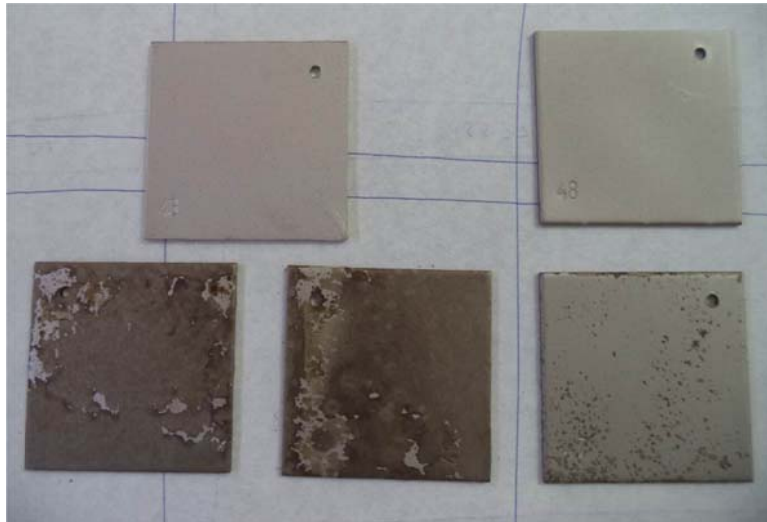
329 thickness of the coating is the same for all the specimens under study after one week
330 of vacuum corrosion testing. Nonetheless, pictures taken at surface level, after the test,
331 show clear damage (Figure 8), even more when this anticorrosive spray is not applied
332 on the specimen. The spray applied is useful to avoid the oxide formation on the
333 surface of the sample under study.

330

Reference   Specimen 1

Specimen 2   Specimen 3 (with anticorrosive spray)

331   **Figure 7. Copper specimens coated with Ni electroless coating**

332

336

337 ## C) Aluminium coated with halar®

340 Figure 9 shows the SEM images captured for each specimen tested under vacuum
341 corrosion test and one reference. The images show the cross section of the specimens
342 under study where halar® coating is shown in the upper side.

344 SEM images revealed that the coating size is exactly the same (around 150 µm) as it is
345 observed in Figure 9. Since neither paths nor holes produced from corrosive products
346 from the TCM are observed, this coating is recommended to be used when in contact
347 with Na_2S/H_2O pair.

345
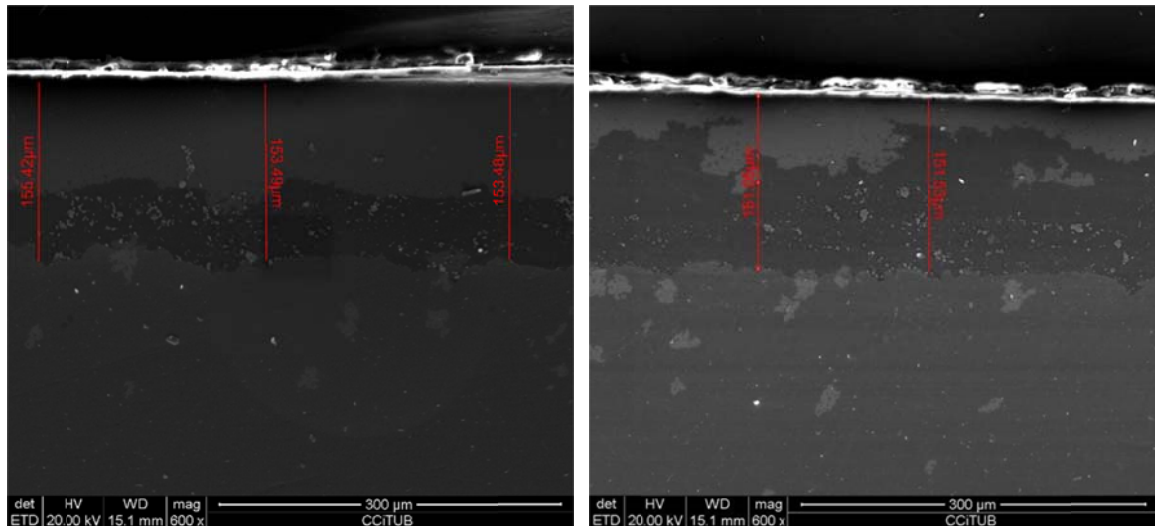
Reference

Specimen 1
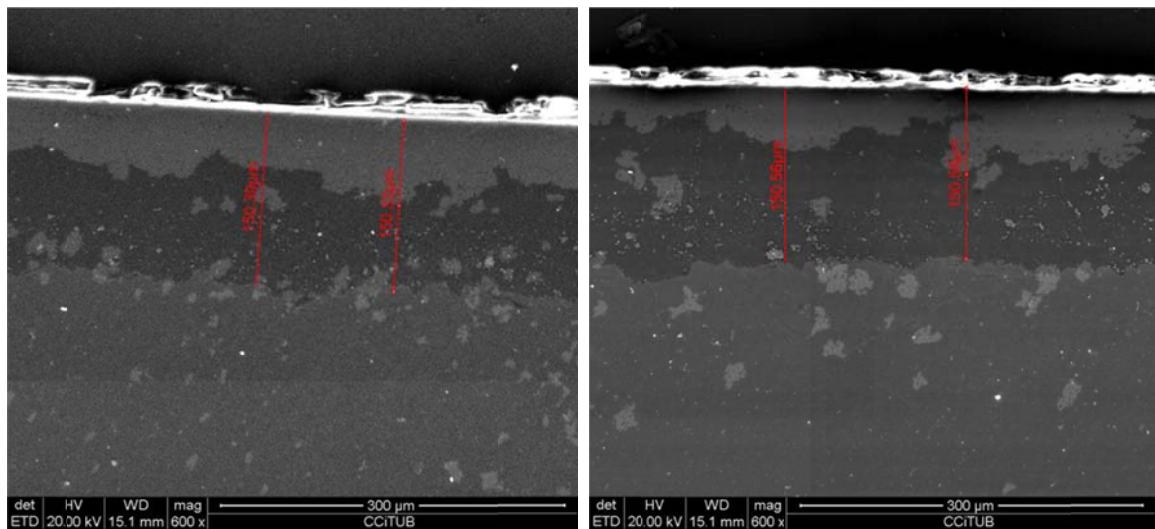
Specimen 2

Specimen 3

Figure 9. Aluminum specimens coated with halar.

346
347

348

349   **D) Aluminium coated with electroless nickel**

356   Results of SEM images of aluminium specimens coated with nickel can be seen in
357   Figure 10. Nickel coating shows a non-flat surface which is in contact with the metal.
358   This fact makes difficult the comparison of the coating thickness. Nevertheless, it can
359   be observed that no corrosion sign is seen since any degradation of the coating,
360   neither inner paths are formed. When specimens are observed visually, as Figure 11, it
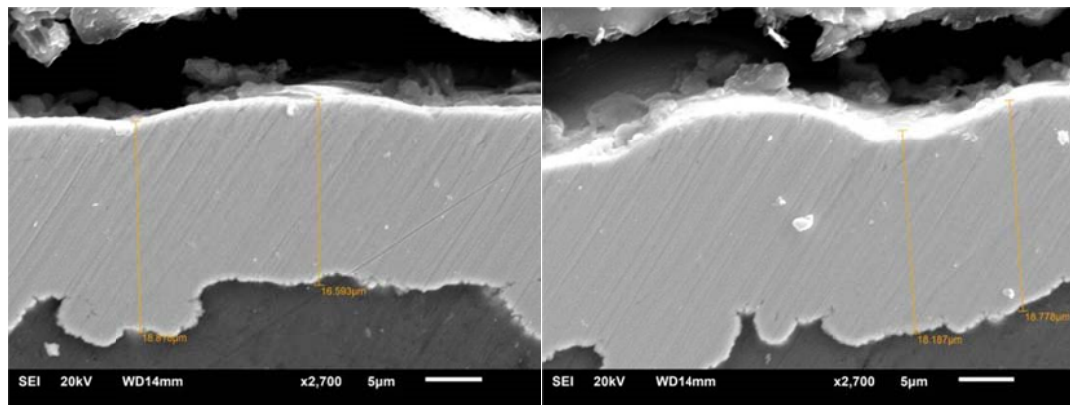361   can be seen that surface is damaged. Therefore, this coating is damaged by Na_2S
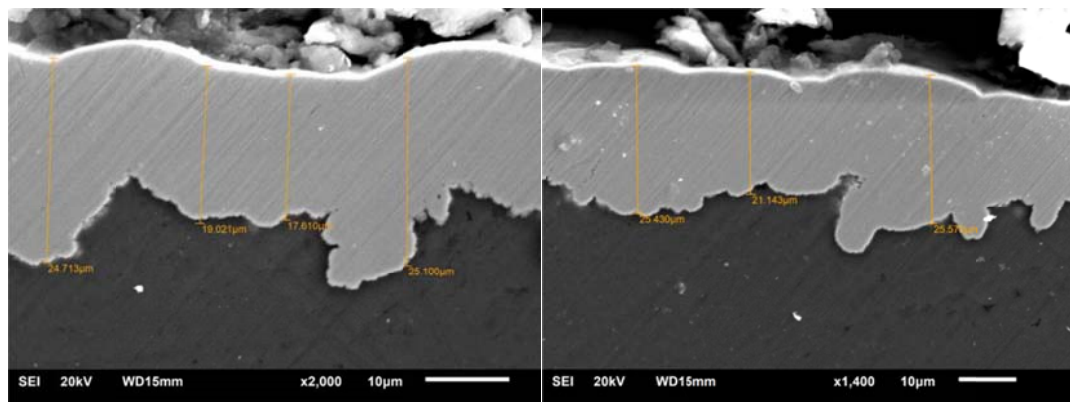362   reaction only at surface level.

357

Reference

Specimen 1

Specimen 2

Specimen 3

Figure 10. Aluminium specimens coated with Ni electroless coating, SEM.

Figure 11. Aluminium specimens coated with Ni electroless coating. On the top, the reference, on the bottom, the three tested specimens.

4.3 Na$_2$S XRD after corrosion vacuum test

X-ray diffraction (XRD) analysis was performed to the TCM after the corrosion vacuum test. This technique shows the crystalline phases that composed the samples. Therefore, the XRD spectrum identifies the crystalline sample components. However, it does not discern the main component, neither quantifies each detected substance.

Here, the aim is to corroborate that the reaction from the nonahydrate to the penthydrate has taken place when performing the vacuum tests. This would imply the appearance of the pentahydrate characteristic peaks in the XRD results.

The XRD spectrum shows that there are three main crystalline substances in this sample: $Na_2S \cdot 5H_2O$, $Na_2S \cdot 9H_2O$ and Na_2SO_3. Na_2SO_3 appears in the composition due to the atmosphere contact during the sample preparation and extraction in the corrosion reactors.

4   Conclusions

A setup composed by a 5 L glass jacketed reactor, evaporator, and a vacuum pump has been developed at lab scale to test corrosion of thermochemical materials under different atmospheres and a wide range of pressure and temperature. A new methodology to perform these tests has been designed, explained in detailed, tested and validated.

One TCM pair, Na_2S/H_2O, has been selected to perform vacuum corrosion tests at 13 mbar and 32.5 ºC when in contact with commonly used metals and coated metals used to build up thermochemical reactors.

From the screening corrosion vacuum tests performed with the TCM reaction from the nonahydrate to the pentahydrate sodium sulphide it can be concluded that copper is not recommended to contain Na_2S/H_2O, neither in open nor in close configurations, besides that in closed and vacuum corrosion rate value is reduced by 30 times. In the case of stainless steel 316 results show that is recommended for long term service.

Two coatings have been tested when applied onto copper and aluminium, two metals highly used for the manufacturing of TCM heat exchangers. Halar coating results make it a potential candidate to be selected to protect heat exchangers/reactor that may contain Na_2S/H_2O pair for thermochemical energy storage. Electroless nickel shows no corrosion when observing SEM images, but it is visually damaged at surface level after the corrosion test. When a finishing spray is applied it improves the material resistance against corrosion.

Moreover, further tests are suggested to carry out to ensure that the materials which do not present corrosion can resist for longer periods. Also, heat transfer coefficient should be measured with the selected metal or coated metal to ensure that heat transfer is not the limiting step in the reactor.

410   **References**

411   [1] International Energy Agency, Technology Roadmap, Energy Storage, 2014.

412   [2] C.W. Chan, J. Ling-Chin, A.P. Roskilly. Reprint of "A review of chemical heat pump,
413   thermodynamic cycles and thermal energy storage technologies of low grade heat
414   utilisation". Appl. Therm. Eng. 53 (2013) 160-176.

415   [3] M.A. Rosen, Energy Storage, Nova Science Publishers, Hauppauge, New York,
416   2012.

417   [4] Y. Aristov, D.M. Chalaev, B. Dawoud, L.I. Heifets, O.S. Popel, G. Restuccia,
418   Simulation and design of a solar driven thermochemical refrigerator using new
419   chemisorbents, Chem. Eng. J. 134, 1, (2007) 58-65.

420   [5]   https://www.nace.org/Publications/Cost-of-Corrosion-Study/   (last   accessed
421   06/06/15)

422   [6] E. Opila, High temperature materials corrosion challenges for energy conversion
423   technologies, Electrochemical Society Interface 22 (2013) 69-73.

424   [7] A. Solé, L. Miró, C. Barreneche, I. Martorell, L. F. Cabeza, Corrosion of metals and
425   salt hydrates used for thermochemical energy storage, Renew. Energ. 75 (2015) 519-
426   523.

427   [8] A. Solé, I. Martorell, L. F. Cabeza, State of the art on gas-solid thermochemical
428   energy storage systems and reactors for building applications, Renew. Sust. Energ.
429   Rev. 47 (2015) 386-398.

430 [9] V.M. Van Essen, J. C. Gores, L.P.J. Bleijendaal, H.A. Zondag, R. Schuitema, M.
431 Bakker, W.G.J. van Helden, Characterization of salt hydrates for compact seasonal
432 thermochemical storage, 3rd International Conference of Energy Sustainability 2009,
433 San Francisco, USA, 19-23 July 2009.

434 [10] X. Fontanet, Estudio del Na_2S como material de almacenamiento termoquímico.
435 University of Barcelona. Graduate Thesis. 2013.

436 [11] A. Frankel, G. Grundmeier, H. McMurray, T. Shinohara, Coatings for corrosion
437 protection, The electrochemical society, New Jersey, US, 2010.

438 [12] A-J. de Jong, R. Stevens, C. Rentrop, C. Hoegaerts, Coating development for
439 thermochemical heat storage reactors, International Conference on Solar Heating and
440 Cooling for Buildings and Industry, SHC 2014, Beijin, China, 2014.

441 [13] S.L. Shawla, R.K. Gupta, Material selection for corrosion control, ASM
442 International, US, 2010.

443 [14] A. Forsgren, Corrosion Control through Organic Coatings, CRC Press, Taylor and
444 Francis Group, US, 2006.

445 [15] J. R. Davis, Corrosion: Understanding the Basics, ASM International, US, 2000.

446 [16] ASTM G1-03, Standard for Preparing, Cleaning, and Evaluating Corrosion Test
447 Specimens. 2003.

448 [17] K. E. N'Tsoukpoe, T. Schmidt, H. U. Rammelberg, B. A. Watts, W.K.L. Ruck, A
449 systematic multi-step screening of numerous salt hydrates for low temperature
450 thermochemical energy storage, Appl. Energ. 124 (2014) 1-16.

451 [18] A-J. de Jong, F. Trausel, C. Finck, L. Van Vilet, R. Cuypers, Thermochemical heat
452 storage – system design issues, International Conference on Solar Heating and
453 Cooling for Buildings and Industry, SHC2013, Freiburg (Germany), Energy Procedia 48
454 (2014) 309-319.

455 [19] www.solvaychemicals.us (last accessed 06/06/15)

456 [20] R. De Boer, W.G. Haije, J.B.J. Veldhuis, Determination of structural,
457 thermodynamic and phase properties in the Na_2S-H_2O system for application in
458 chemical heat pump, Thermochim. Acta 395 (2003) 3-19.

459 [21] D. L. Perry, Handbook of inorganic compounds, second ed., CRC Press, 2011.

460   [22] www.alfa.com/msds/british/11664.pdf (last accessed 06/06/2015)

461   [23] M. Kutz, Applied Plastics Engineering Handbook: Processing and Materials, Hand

462   Book Series, Elsevier, US, 2011.

463   [24] K.L. Choy, Chemical vapour deposition of coatings, Prog. Mater. Sci. 48, 2 (2003)

464   57–170.

465   [25] ASTM B 733 – 97, Standard Specification for Autocatalytic (Electroless) Nickel-

466   Phosphorus Coatings on Metal, 1997.

467   [26] V.S. Sastri, E. Ghal, M. Elboujdaini, Corrosion, prevention and protection. Practical

468   solutions, John Wiley & Sons, Chichester, UK, 2007.